Phys. Lett. B 847 (2023) 138283

Contents lists available at ScienceDirect

Physics Letters B

journal homepage: www.elsevier.com/locate/physletb

Letter

Neutron polarisation transfer, $C_{x'}$, in π^+ photoproduction off the proton, $d(\gamma^{\odot}, \vec{n}\pi^+)n_{spec}$

M. Bashkanov [a,*], D.P. Watts [a], S.J.D. Kay [b], S. Abt [e], P. Achenbach [f], P. Adlarson [f], F. Afzal [g], Z. Ahmed [b], C.S. Akondi [c], J.R.M. Annand [d], R. Beck [g], M. Biroth [f], N. Borisov [h], A. Braghieri [i], W.J. Briscoe [j], F. Cividini [f], C. Collicott [k], S. Costanza [l,i], A. Denig [f], E.J. Downie [j], P. Drexler [m,f], S. Fegan [a], A. Fix [r], S. Gardner [d], D. Ghosal [e], D.I. Glazier [d], I. Gorodnov [h], W. Gradl [f], D. Gurevich [n], L. Heijkenskjöld [f], D. Hornidge [o], G.M. Huber [b], V.L. Kashevarov [f,h], M. Korolija [p], B. Krusche [e], A. Lazarev [h], K. Livingston [d], S. Lutterer [e], I.J.D. MacGregor [d], D.M. Manley [c], P.P. Martel [f,o], R. Miskimen [q], E. Mornacchi [f], C. Mullen [d], A. Neganov [h], A. Neiser [f], M. Ostrick [f], P.B. Otte [f], D. Paudyal [b], P. Pedroni [i], T. Rostomyan [e], V. Sokhoyan [f], K. Spieker [g], O. Steffen [f], I.I. Strakovsky [j], T. Strub [e], I. Supek [p], A. Thiel [g], M. Thiel [f], A. Thomas [f], Yu.A. Usov [h], S. Wagner [f], N.K. Walford [e], J. Wettig [f], M. Wolfes [f], R.L. Workman [j], N. Zachariou [a]

[a] Department of Physics, University of York, Heslington, York, Y010 5DD, UK
[b] University of Regina, Regina, SK S4S-0A2 Canada
[c] Kent State University, Kent, OH 44242, USA
[d] SUPA School of Physics and Astronomy, University of Glasgow, Glasgow, G12 8QQ, UK
[e] Department of Physics, University of Basel, CH-4056 Basel, Switzerland
[f] Institut für Kernphysik, University of Mainz, D-55099 Mainz, Germany
[g] Helmholtz-Institut für Strahlen- und Kernphysik, University Bonn, D-53115 Bonn, Germany
[h] Joint Institute for Nuclear Research, 141980 Dubna, Russia
[i] INFN Sezione di Pavia, I-27100 Pavia, Italy
[j] Center for Nuclear Studies, The George Washington University, Washington, DC 20052, USA
[k] Department of Astronomy and Physics, Saint Mary's University, E4L1E6 Halifax, Canada
[l] Dipartimento di Fisica, Università di Pavia, I-27100 Pavia, Italy
[m] II. Physikalisches Institut, University of Giessen, D-35392 Giessen, Germany
[n] Institute for Nuclear Research, RU-125047 Moscow, Russia
[o] Mount Allison University, Sackville, New Brunswick E4L1E6, Canada
[p] Rudjer Boskovic Institute, HR-10000 Zagreb, Croatia
[q] University of Massachusetts, Amherst, MA 01003, USA
[r] Tomsk Polytechnic University, 634034 Tomsk, Russia

ARTICLE INFO

Editor: M. Doser

Keywords:
Photoproduction

ABSTRACT

We report a first measurement of the double-polarisation observable, $C_{x'}$, in π^+ photoproduction off the proton. The $C_{x'}$ double-polarisation observable represents the transfer of polarisation from a circularly polarised photon beam to the recoiling neutron. The MAMI circularly polarised photon beam impinged on a liquid deuterium target cell, with reaction products detected in the Crystal Ball calorimeter. Ancillary apparatus surrounding the target provided tracking, particle identification and determination of recoil nucleon polarisation. The $C_{x'}$ observable is determined for photon energies 800-1400 MeV, providing new constraints on models aiming to elucidate the spectrum and properties of nucleon resonances. This is the first determination of any polarisation observable from the beam-recoil group of observables for this reaction. Inclusion of the new data in the database of the SAID partial wave analysis shifted the solution to a new global minima which, not only gives better agreement with

* Corresponding author.
E-mail address: mikhail.bashkanov@york.ac.uk (M. Bashkanov).

https://doi.org/10.1016/j.physletb.2023.138283
Received 17 November 2022; Received in revised form 24 August 2023; Accepted 24 October 2023
Available online 28 October 2023

the current data, but also improves the description of a range of other single and double polarisation observables for charged pion photoproduction.

1. Introduction

Photoinduced reactions on proton and neutron targets have played a key role in progressing our knowledge of the excited nucleon spectrum in the past decade [1], catalysed by quality nucleon photoproduction data from MAMI, JLab, ELSA, SPring-8, ELPH and other facilities [2,3]. These have provided a step change in the number of measured observables, statistical accuracy, and kinematic coverage.

Pion photoproduction is the simplest photoinduced reaction on the nucleon. The reaction can be described theoretically with four complex amplitudes, which can be fully constrained, up to an overall phase, by kinematically complete measurements of a chosen set of eight observables taken from the cross section, single polarisation observables (where the polarisation of either photon beam, target or recoiling nucleon is determined) and double-polarisation observables formed from simultaneous determination of two of the above polarisation quantities. Recent work has indicated that the properties of the different partial waves in the reaction may converge with fewer measurements than the mathematically complete eight, as discussed in Ref. [4].

Previous double-polarisation measurements for $n\pi^+$ photoproduction are limited to the beam-target group of observables. Measurements of the G observable (linearly polarised beam and transversely polarised target) [5], the E observable (circularly polarised beam and longitudinally polarised target [6]) and more limited data sets for H (circularly polarised beam and transversely polarised target) have recently been obtained [7,8]. These double-polarisation data, combined with the cross section and single polarisation observables (Σ, T and P) [5,9] comprise the current world data base for $n\pi^+$ photoproduction.

The lack of any double-polarisation measurements from the beam-recoil group for this channel means the mathematically "complete" constraint has not been achieved. This lack of previous data reflects the challenges in measuring the recoil nucleon polarisation, requiring a secondary rescattering of the ejectile nucleon in a spin-analysing polarimeter material. Such measurements are only feasible at high photon beam intensities.[1] The new $C_{x'}$ data presented here therefore provide experimental constraint on amplitude combinations for $n\pi^+$ not currently present in the database, with the potential to shift the PWA solutions to a different global minima. In addition, the ability of current PWA to describe this new data, when only constrained by double-polarisation data from a different observable group, are an important cross check of the convergence of PWA analyses in the absence of beam-recoil data and also an independent constraint on systematics in the current database.[2] Even if the beam-recoil observables are determined with less precision than the beam-target measurements which dominate the database, their sensitivity to poorly constrained amplitude combinations have the potential to influence the true global minima extracted in PWA.

The photoproduction of $p\pi^0$ is the sister reaction to $n\pi^+$. For the $p\pi^0$ reaction the database is more complete. The differential cross-section, $\Sigma, P, T, G, H, C_{x'}$ observables have been determined over the full energy range of the new data and $E, O_{x'}, O_{z'}$ for part of the range.[3] Such $p\pi^0$ data are simultaneously fitted by theoretical models along with the $n\pi^+$ data. In combination, sensitivities to the isospin of the contributing nucleon resonances and backgrounds can be achieved.

The leading phenomenologies to interpret pion photoproduction data, and infer information on the nucleon resonance spectrum, are the SAID [9] and BnGa [10] frameworks, which are both based on partial wave analysis (PWA) methods fitted to the data. The latest iterations of descriptions (SAID SM22 [8] and BnGa BG2019 [7]) experienced substantial change due to the inclusion of new data on the double-polarisation observable G, recently measured at CLAS [5].

Given the topic of the current paper, it is informative to look at the current status of $C_{x'}$ measurement for the sister $p\pi^0$ and compare with the latest PWA solutions. These $p\pi^0$ data (A2@MAMI [29] and Hall-A@JLab [30]) comprised (prior to the current work) the only measurements of beam-recoil observables obtained in pion photoproduction. The A2@MAMI data was obtained with a preliminary polarimeter apparatus (which lacked the particle tracking capabilities of the new system). Both datasets are shown on Fig. 3 compared to the latest PWA solutions. Despite the $p\pi^0$ channel having a large database of double-polarisation observables (larger than for the other 3 channels combined) there remains a sizeable difference between the PWA solutions, even in the region of the Δ, illustrating the different sensitivities of this observable in PWA.

In this work we make a first determination of the $C_{x'}$ observable for the $p(\gamma^{\odot}, \vec{n}\pi^+)$ reaction, obtained from a month long beamtime on a deuterium target. The experiment incorporated a new nucleon recoil polarimeter which enabled recoil polarisation observables in pion photoproduction from both proton and neutron channels to be measured with common apparatus and without prohibitively long beamtimes. This is the first measurement of any observable from the beam-recoil double polarisation group for this reaction and the results are compared to predictions from the leading partial wave analysis based theoretical models. The data analysis methodologies are also improved compared to the earlier work [29]. The $C_{x'}$ observable is extracted using a bootstrap statistical technique which gives access to statistical and systematic uncertainties in a more robust way. We compare the new data to the SAID [9] and BnGa [10] partial wave analysis, which are fitted to a database currently unconstrained by measurements of beam-recoil observables in this reaction channel. As an initial exploration of the impact of the new data, an updated SAID solution was obtained by fitting to the world database including this $C_{x'}$ data. A new minima in the PWA solution is found. The quality of the fit of this new solution to the $C_{x'}$ data is presented, as well as a discussion of the impact on the description of other observables in the database from this new solution.

2. Experimental details

The measurement employed a new, large acceptance, neutron polarimeter [11] within the Crystal Ball detector at the A2@MAMI [12] facility during a 600 hour beamtime. A 1557 MeV longitudinally polarised electron beam impinged on either a thin amorphous (cobalt-iron alloy) or crystalline (diamond) radiator, producing circularly (alloy) or elliptically (diamond) polarised bremsstrahlung photons. The electron helicity was regularly flipped to produce a photon beam with equal amounts of both circular photon polarisations. As linear photon beam polarisation is not used to extract $C^n_{x'}$, equal flux from the two elliptical

[1] To achieve such measurements around four orders of magnitude larger statistics are required than for a typical beam-target measurements as only ~2% of the ejected events can be analysed with a practical thickness of nucleon scattering medium.

[2] For example, correlated systematics could potentially arise as all the beam-target observables employed common methodologies in determining the degree of linear beam polarisation and MAMI/ELSA had common polarised target systems.

[3] Note: there is also $C_{z'}$ data for $p\pi^0$ but only for a limited set of discrete angles.

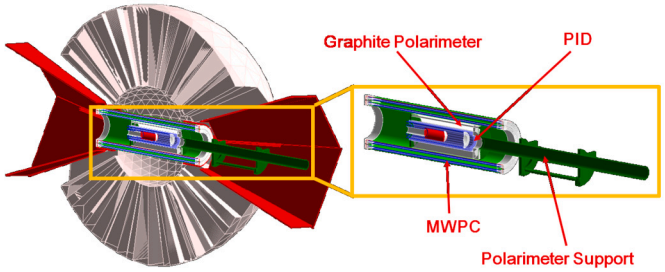

Fig. 1. Crystal Ball setup during the polarimeter beamtime. The cryogenic target (red cell) is surrounded by the PID barrel (blue), the graphite polarimeter (grey), the MWPC (blue/green) and the Crystal Ball (white).

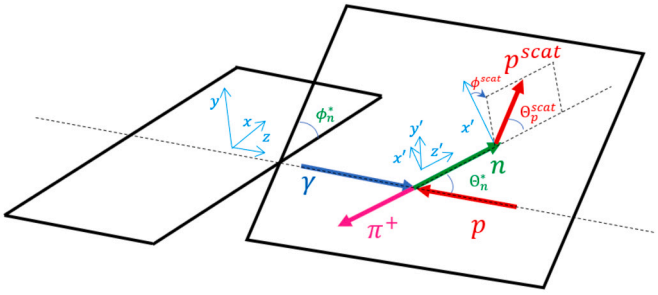

Fig. 2. Kinematics of the reaction in the centre-of-mass system. The z-axis is oriented along the photon beam, the y-axis is vertically upwards in the laboratory; the z'-axis is oriented along the ejectile neutron direction, and the y'-axis is perpendicular to the reaction plane.

polarisation settings were combined to increase the circularly polarised photon yield.[4] The photons were energy-tagged ($\Delta E \sim$ 2 MeV) by the Glasgow-Mainz Tagger [13] and impinged on a 10 cm long liquid deuterium target cell. Reaction products were detected by the Crystal Ball (CB) [14], a highly segmented NaI(Tl) photon calorimeter covering nearly 96% of 4π steradians. For this experiment, a new bespoke 24 element, 7 cm diameter and 30 cm long plastic scintillator barrel (PID-POL) [15–17] surrounded the target, with a smaller diameter than the earlier PID detector [15], but which provided similar particle identification capabilities. A 2.6 cm thick cylinder of analysing material (graphite) for nucleon polarimetry was placed around PID-POL, covering polar angles $12° < \Theta < 150°$ and occupying the space between PID-POL and the Multi Wire Proportional Chamber (MWPC) [18]. The MWPC provided charged particle tracking for particles passing out of the graphite into the CB. At forward angles, an additional 2.6 cm thick graphite disk covered the range $2 < \Theta < 12°$ [15–17]. A GEANT4 visualisation of the experimental setup can be seen in Fig. 1.

The cryogenic deuterium target provided a source of weakly bound protons and neutrons. The $d(\gamma,\pi^+\vec{n})n_{spec}$ events of interest consist of a primary charged pion track and a reconstructed neutron, which undergoes a (n,p) charge-exchange reaction in the graphite to produce a secondary proton; the spectator neutron is not detected. The secondary proton gives signals in the MWPC and CB. The primary π^+ was identified using the correlation between the energy deposits in the PID and CB using $\Delta E - E$ analysis [15] along with an associated charged track in the MWPC. The intercept of the primary π^+ track with the photon beamline allowed determination of the production vertex, and hence permitted the yield originating from the target cell windows to be removed. Neutron ^{12}C(n,p) charge exchange candidates required an absence of a PID-POL signal on the reconstructed neutron path, while having an associated track in the MWPC and signal in the CB from the scattered secondary proton. The incident neutron angle (Θ_n) was determined from reaction kinematics using E_γ and the production vertex coordinates. A distance of closest approach condition was imposed to ensure a crossing of the (reconstructed) neutron track and the secondary proton candidate track (measured with MWPC and CB). Once candidate pion and neutron tracks were identified, a kinematic fit was employed to increase the purity of the data sample and improve the determination of the reaction kinematics (see Ref [19] for details).

3. Determination of $C_{x'}$

The cross section for pion photodisintegration by circularly polarised photons with determination of recoil neutron polarisation is given [20] by:

$$\frac{d\sigma}{d\Omega} = \left(\frac{d\sigma}{d\Omega}\right)_0 \cdot [1 + C^n_{x'} \cdot P^\odot_\gamma \cdot A \sin(\phi^{scat}) + P_y A \cos(\phi^{scat})], \quad (1)$$

where $\left(\frac{d\sigma}{d\Omega}\right)_0$ is the unpolarised cross-section, $C^n_{x'}$ is the transferred polarisation from the photon to the recoiling neutron, $P^\odot_\gamma$ is the circular polarisation of the incoming photon (which in our case is flipped between positive and negative values) and A is the analysing power for the ^{12}C(n,p) reactions occurring in a graphite analysing medium (the polarimeter). P_y is the (helicity independent) induced nucleon polarisation. ϕ^{scat} is the azimuthal angle of the scattered proton from ^{12}C(n,p) in the primed frame, where the z-axis is in the direction of the nucleon and the x and y axes are defined relative to the reaction plane (see Fig. 2).

To extract $C^n_{x'}$ from the measured data a log-likelihood ansatz was employed. The event-by-event likelihood function, proportional to the event yield (the product of cross section and acceptance), can be defined as:

$$L_i = c_i \left[1 + A_{y,i}(C^n_{x'} \cdot P^\odot_{\gamma,i} \cdot \sin(\phi^{scat}_i) + P_y \cos(\phi^{scat}))\right] A_i, \quad (2)$$

where i is the index of the event under consideration, c_i is a normalization coefficient, A_i is the detector acceptance. $A_{y,i}$ is the analysing power for the ^{12}C(n,p) reaction for the kinematics of the event (i).

The experimental dataset, comprising i events, is fitted by a log-likelihood function, obtained by taking the log of equation (2):

$$\log L = b + \sum_i \log\left[1 + A_{y,i}(C^n_{x'} \cdot P^\odot_{\gamma,i} \cdot \sin(\phi^{scat}_i + P_y \cos(\phi^{scat}))\right]. \quad (3)$$

The summation (i) reflects how the function is minimised by fitting to all data. The fit has free parameters b and $C^n_{x'}$, while $P^\odot_{\gamma,i} \cdot A_{y,i}$ are fixed and calculated on an event-by-event basis. P_y is helicity independent and was taken from Ref [10]. The extracted $C^n_{x'}$ is rather insensitive to the adopted value of P_y giving maximum variation of 0.02. The constant b is an observable-independent constant, which absorbs the normalization coefficient and detector acceptance, but whose contribution cancels in the likelihood extraction of $C^n_{x'}$ (derived from an asymmetry of yields between the two beam helicity states which are flipped regularly with a period of $\sim 1s$).

The fitting procedure used unbinned azimuthal scatter distributions to mitigate any bin-size dependent systematic effects. The spin transfer observable, $C_{x'} = f(\Theta^*_N, E_\gamma)$, was determined in 10° neutron centre-of-mass (CM) angle bins using a likelihood-extraction in which a smooth energy dependence is assumed.[5] To ensure accurate calculation of the uncertainties in extraction of $C_{x'}$, where there is potential for correlated uncertainties, we employ a bootstrap technique [21]. From our sample of N events we randomly select N events, allowing repetitions,[6] and make a likelihood fit to extract $C_{x'}$ as a function of the energy, $C_{x'} =$

[4] Separate treatment of the events with two elliptical photon polarisations and with pure circular photon polarisation, gave consistent results within the achievable statistical accuracy.

[5] In this particular case smooth functions were parameterised by equidistant (200 MeV apart) Gaussians with fixed 100 MeV σ and arbitrary strength. To avoid biases, the central values of Gaussians were randomised for each bootstrap cycle.

[6] For example, in the case of the 80° bin it is 9200 random events out of a 9200 event sample.

$f(E_\gamma)$.[7] Multiple repetitions of the procedure provide the most likely $C_{x'}$ along with determination of the associated statistical and systematic uncertainties.[8]

The fixed parameters in the likelihood fit to the data (equation Eq. (2)) are $P^{\odot}_{\gamma,i}$ and $A_{y,i}$, which are both determined on an event-by-event basis. $P^{\odot}_{\gamma,i}$ is calculated analytically from the incident electron beam energy and the tagged photon energy [22]. The systematic uncertainty in helicity polarisation from the calculation is estimated [23] to be 3%. The magnitude of $A_{y,i}$ depends on the ejectile neutron energy and scattered proton polar angle for the identified ^{12}C(n,p) reaction. The $A_{y,i}$ for each event was taken from the SAID parameterisation [8] of free n-p scattering, modified to account for the n-p reactions occurring in ^{12}C using an experimental determination of A_y for ^{12}C$(n,p)X$ by JEDI@Juelich [24]. The magnitude of the SAID analysing powers were calibrated to the JEDI data by the function: $A_y(n^{12}C)/A_y(np) = 1+e^{(1.82-0.014E_n[MeV])}$. This modified analysing power function described the JEDI data with a χ^2 close to 1. The enhancement originates from the contribution of coherent nuclear processes, such as ^{12}C$(n,p)^{12}$N. For the lowest photon energies sampled, in the Δ region, the typical neutron analysing power is enhanced over the SAID prediction by ~30%. The size of the enhancement reduces with increasing photon (neutron) energy *e.g.* it is below ~5% for E_γ above 1.0 GeV. The angular distributions from the SAID predictions agreed with the JEDI data. To avoid regions of low analysing power, events were only retained for analysis if $A_y(np) \geq 0.1$ and the proton polar scattering angle relative to the direction of the neutron, Θ_p^{scat}, was in the range 15-45°. The above cuts restrict the kinetic energy of the neutrons to be above 200 MeV, as well as their polar angle, Θ_n, to be larger than ~ 40°. The systematic uncertainty of the analysing power determination is derived from the uncertainty of the JEDI ^{12}C$(n,p)X$ measurement to which it is calibrated (estimated to be 10%[9]).

Relaxing the analysis cuts gave negligible change in the extracted $C_{x'}$ (absolute changes below 0.02). The consistency of $C_{x'}$ extraction from separated amorphous and diamond radiator datasets gave the dominant contribution to the systematic uncertainties budget (typically 0.2 for much of the parameter space). However the magnitude of this uncertainty is driven by the available statistics, and could be reduced in future measurements.

The measurement was performed for protons bound in deuterium while the event reconstructions assumed a stationary proton. The systematics of this approximation were explored. A simulation, utilising a Hulthen wave function for the protons in deuterium [26] allowed the error in $C_{x'}$ extraction due to the assumption of a stationary proton to be assessed. For the energy range of interest, the systematic uncertainty is $\sigma[\%] = 0.5 + 6.2/E_\gamma[GeV]$ - corresponding to around 8% for $E_\gamma = 800$ MeV and dropping to ~ 5% for $E_\gamma = 1400$ MeV.

The measurement of proton photoreactions from a deuteron target can also be sensitive to effects from nucleon Final-State-Interactions (FSI). It was also shown in Ref. [27,28] that such FSI effects contribute weakly for charged-pion photoproduction, *i.e.*, π^+nn and π^-pp channels, and are expected to be below 5% for the $C_{x'}$ observable for the photon energies sampled here, which we took as a conservative estimate of this systematic uncertainty.

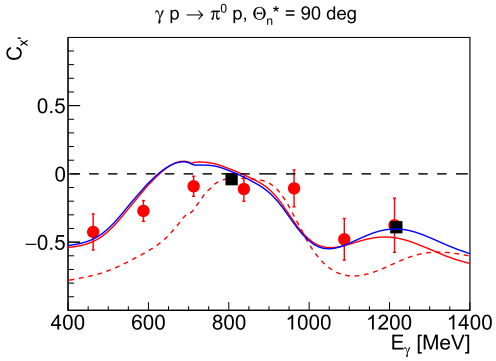

Fig. 3. $C_{x'}$ observable data for the $p\pi^0$ reaction from A2@MAMI, Ref. [29] (red circles) and Hall-A@JLab Ref. [30] (black squares), together with SAID-SM22 [9] (solid red), SAID-BA23 (solid blue) and BnGa-19 [5] (dashed red) predictions.

Table 1
A tabulated summary of the systematic uncertainties. Note that depending on the source of the systematic error they are quoted either as absolute uncertainties or as a percentage of the measured $C_{x'}$.

Type	uncertainty
$P^{\odot}_{\gamma}$	3%
$A_y(^{12}$C$(n,p)X)$	10%
quasi-free measurement	variable ~ 6.5%
FSI contribution	5%
selection cuts	0.02
P_y	0.02
amorphous/diamond	variable ~ 0.2

Typical magnitudes of each of the systematic uncertainties are summarised in Table 1. These systematic uncertainties, and their kinematic dependencies, are combined in quadrature to obtain the total bin-dependent systematic uncertainty, presented with the experimental data as an error band in Fig. 4.

4. Results

Our $C_{x'}$ results for the $n\pi^+$ channel are presented in Fig. 4 as a function of photon energy (E_γ = 800-1400 MeV) and in 5° bins of neutron CM polar angle covering 70-120°.[10] The associated statistical (systematic) uncertainties are shown by the dark grey bands (hatched bands on the x-axis), respectively. The combined error is shown by the light grey band. The extracted $C_{x'}$ for the more forward angles below ~95° is small and broadly uniform. For more backward angles a peak-like structure around E_γ = 1000-1400 MeV is suggested by the new data.

Fig. 4 also shows comparisons of the new $C_{x'}$ data with the most recent solutions of the SAID-SM22 (red solid) [9] and BnGa (red dashed) [5] partial wave fits. These solutions include the recent precision measurements of the beam-target observables (G and E) for this channel, which span E_γ = 0.7 to 2.3 GeV, covering the entire photon energy range presented in Fig. 4 [5].

The predictions below E_γ ~800 MeV are outside of the acceptance of the current data, but are worthy of discussion. The different PWA for $C_{x'}$ show broad convergence. However, SAID-SM22 tends to predict larger values than BnGa, with the largest differences evident at forward

[7] For example if we have only 5 events (0,1,2,3,4) we randomise the sample and get another set of 5 events which consist of (1,3,0,1,3) and make a fit on this set. Events 1 and 3 appear twice, events 2 and 4 did not appear at all. We iterate this procedure multiple times and the resulting distribution of fit outcomes would peak at the most probable $C_{x'}$ with the width of the distribution corresponding to the $C_{x'}$ uncertainty.

[8] The dataset corresponds to kinematical regions where $C_{x'}$ statistical uncertainties are less than 0.5 or systematical uncertainties are smaller than 0.8.

[9] The JEDI ^{12}C(n,p) data are unpublished. The systematic error can be obtained from the published ^{12}C(d,d) analysing power measurement, which used common apparatus and the same beamtime. In this, the systematic uncertainty is shown to be dominated by the uncertainty in beam polarisation which is established to be 10% [25]).

[10] Note that BnGa and SAID adopt opposite sign for this observable [31]. In our work we adopt the same conventions as BnGa. Also both BnGa and SAID databases show $C_{x'}$ observable as a function of pion angle [31].

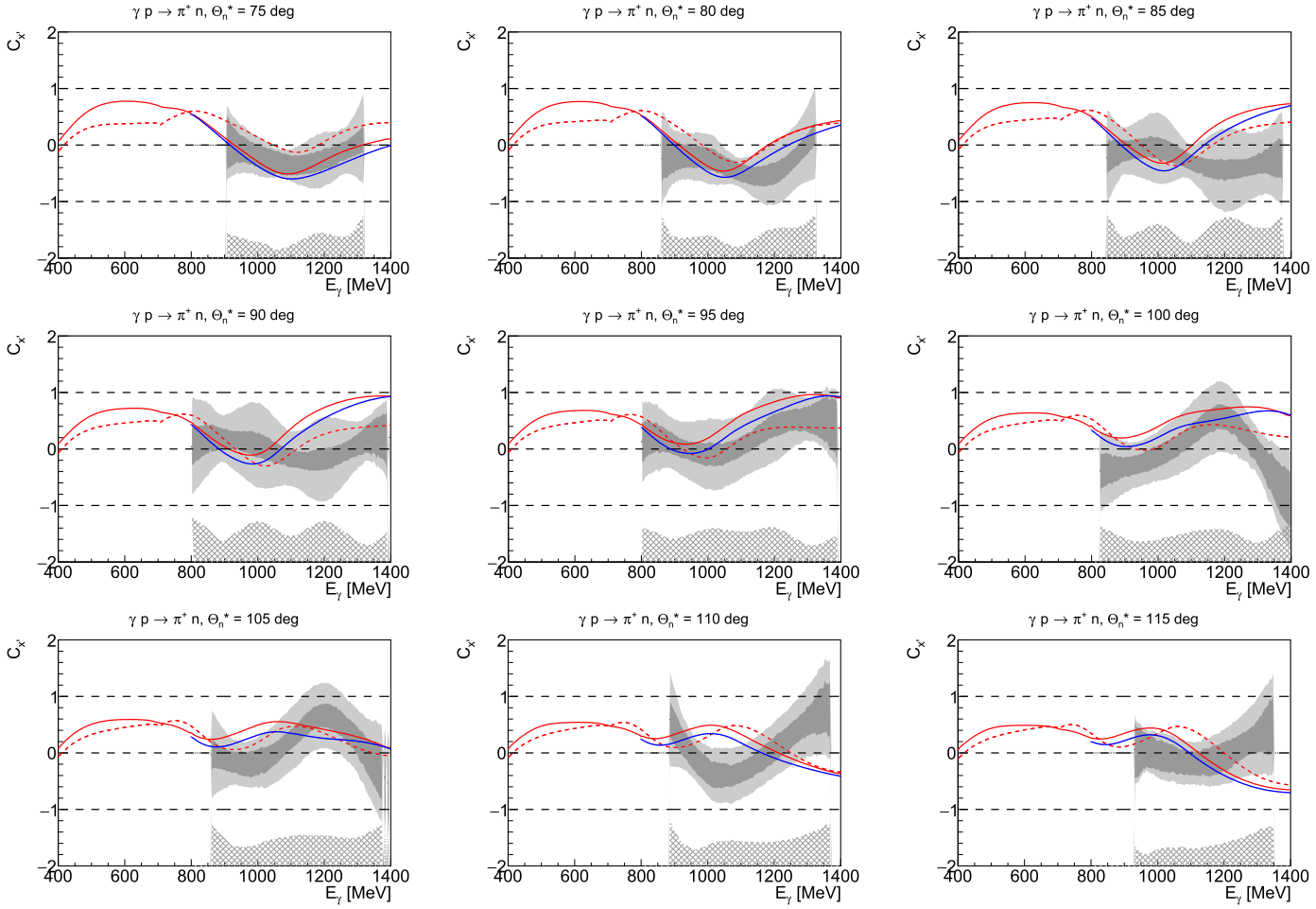

Fig. 4. The neutron spin transfer observable $C_{x'}$ for the 75° – 115°, neutron CM angles as a function of photon beam energy. The dashed dark grey area represents the data together with its statistical uncertainty, while the hatched area shows the systematic uncertainty. Statistical and systematical uncertainties added in quadrature are shown as light grey band. The solid red line is a latest SAID-SM22 [9] PWA solution; the dashed red line is a latest BnGa-19 [5] solution. The solid blue line showed SAID-BA23 fit after inclusion of current $C_{x'}$ data.

angles.[11] It is interesting that even in the well studied region near the Δ resonance there remain differences between PWA predictions. Clearly future $C_{x'}$ measurements in this region would provide valuable new information for PWA.[12] We remark that the current BnGa solution did not describe the $p\pi^0$ $C_{x'}$ data in this region (Fig. 3) so it would seem appropriate to compare PWA convergence in $C_{x'}$ with an updated fit database.

Above $E_\gamma \sim 800$ MeV comparisons of the PWA with the new data can be made. For the region $E_\gamma \sim 800 - 1100$ MeV both PWAs describe the data within the combined errors for the majority of the angle bins. The two PWA predictions are broadly consistent in this region, except at more forward angles where they predict a different sign. Above $E_\gamma \sim 1100$ MeV the PWA show clear discrepancies with the data for a number of the different angular bins. The differences tend to be more pronounced at the highest E_γ ~1300-1400 MeV region where, for some angular bins, both PWA predict an opposite sign for $C_{x'}$ than evident in the new data. Neither PWA shows significant evidence for the peak-like structure around E_γ = 1000-1400 MeV suggested by the new data in the ~100-110° range.

Clearly these new $C_{x'}$ data will be valuable to improve convergence between PWAs, and potentially improve the extracted properties of the contributing resonances and backgrounds. We remark that the highest photon energies sampled here, around 1400 MeV, correspond to CM energies of $W = 1.872$ MeV - where quark models and LatticeQCD predict a high density of resonant states, many of which are poorly established experimentally [33].

As a first assessment of the impact of the new data, they have been included in the SAID database and a new fit was extracted[13] (SAID-BA23). A summary of the overall quality of fit for SAID-BA23 solutions to the new $C_{x'}$ data as well as the complete database for all pion photoproduction channels is shown in Table 2. For SAID-BA23 the goodness of fit (χ^2/data) of the new $C_{x'}$ data is improved by around 40% over the previous solution (SAID-SM22). However, the new solution also shows improved agreement with the current database of all other pion production channels, with the largest improvement (22%) observed for $p\pi^-$. For specific observables in the databases, the greatest shifts in fit quality were seen for the beam spin asymmetry Σ and G observables in $n\pi^+$ and the Σ and T data in $p\pi^-$. An example, the improved description of the target polarisation observable, T, is shown in Fig. 5.

[11] The structure around $E_\gamma \sim 700$ MeV originates from the η-meson production threshold.

[12] A dedicated 5 week beamtime with a lower electron beam energy than the current work, $E_e = 855$ MeV, was obtained in early 2023 (currently under analysis) and will provide such data.

[13] To implement the $C_{x'}$ data into the SAID database, the energy unbinned results were binned into 5 MeV bins, which resulted in 920 new data points. This initial fit included only the statistical errors of the new data.

Table 2
$\gamma N \to N\pi$ SAID fit quality ($E_\gamma \in [800, 1400]$ MeV).

Fit	$p\pi^0$(3142)	$n\pi^0$(240)	$n\pi^+$(1133)	$p\pi^-$(779)	$C_{x'}$ (920[a])	
	$\chi^2/data$	$\chi^2/data$	$\chi^2/data$	$\chi^2/data$	$\chi^2/data$ σ_{stat}	$\chi^2/data$ σ_{full}
CM12	5.70	6.33	6.27	29.07	6.43	1.05
SM22	2.29	6.30	3.11	2.08	5.43	0.84
BA23	**2.11**	**6.13**	**2.92**	**1.70**	**3.90**	**0.65**

[a] Number in parentheses displays datapoints in each dataset.

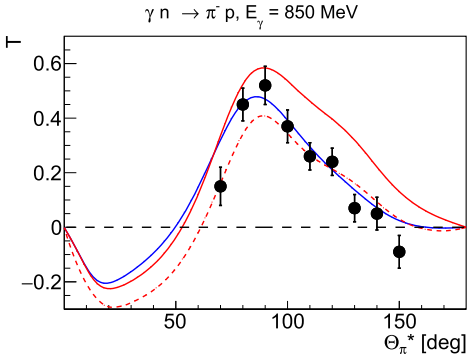

Fig. 5. T observable data from Bonn, Ref. [32], together with SAID-SM22 [9] (solid red), SAID-BA23 (solid blue) and BnGa-19 [5] (dashed red) fits.

The predictions of $C_{x'}$ from SAID-BA23 are shown by the solid blue curves on Fig. 4. Although the overall description of the data is improved it is clear that the solution does not accurately describe the new data over the full energy and angular range. This is particularly evident at the higher photon energies where constraints from other measurements in the database appear to provide tight constraints on $C_{x'}$ in all the different variants. The most recent prediction from the Bonn-Gatchina group (BnGa-19) is shown by the red-dash line. This shows convergence with SAID in $C_{x'}$ for the highest energies and angles. For smaller angles, below ~100°, it tends to show better agreement with the data in this higher E_γ region.

As $C_{x'}$ constrains different combinations of production amplitudes than the other observables in the database, it would be worthwhile to carry out studies of weighting the new data in the partial wave analysis fits and systematically exploring the effect on the extracted partial waves and the predictions of observables for other channels. Such studies will be presented in a future publication.

We remark that the statistical and systematic uncertainties in the $C_{x'}$ extraction could be significantly reduced in the future due to upgrades in the MAMI beam intensity since the data was obtained. The current results suggest that beam-recoil data can significantly influence the true global minima in PWA even when, as is the case here, an extensive database of single polarisation and beam-target double-polarisation observables has already been obtained.

5. Summary

This work provides the first measurement of a beam-recoil double-polarisation observable, $C_{x'}$, for $n\pi^+$ photoproduction off the proton, obtained for photon energies 800-1400 MeV. The measurement provides new constraints on the leading partial wave analysis based models which fit the world data on photo-meson production from the nucleon to extract the nucleon excitation spectrum. A fit including the data using the SAID partial wave analysis framework (SAID-BA23), as expected, improved the description of the new $C_{x'}$ data. However, the new fit simultaneously improved the description of the databases for all other pion photoproduction channels. The largest improvement in χ^2, a 22% decrease, was observed in the fit of the $p\pi^-$ database, with notable improvements to the description of target polarisation, T, and beam spin asymmetry, Σ. This highlights how beam-recoil observables such as $C_{x'}$, even when obtained with poorer statistical accuracy than other observables, influence the solutions of partial wave analysis because of their differing sensitivities to the basic complex reaction amplitudes.

Declaration of competing interest

The authors declare that they have no known competing financial interests or personal relationships that could have appeared to influence the work reported in this paper.

Data availability

Data available under link of Ref. [23].

Acknowledgements

In accordance with UK data management policy, all data are available for downloading from PURE [34]. This work has been supported by the U.K. STFC (ST/V002570/1, ST/L00478X/2, ST/V001035/1, ST/P004385/2, ST/T002077/1, ST/L005824/1, 57071/1, 50727/1) grants, the Deutsche Forschungsgemeinschaft (SFB443, SFB/TR16, and SFB1044), DFG-RFBR (Grant No. 09-02-91330), Schweizerischer Nationalfonds (Contracts No. 200020-175807, No. 200020-156983, No. 132799, No. 121781, No. 117601), the U.S. Department of Energy (Offices of Science and Nuclear Physics, Awards No. DE-SC0016583, DE-SC0016582, DE-SC0014323, DEFG02-99-ER41110, No. DE-FG02-88ER40415, No. DEFG02-01-ER41194) and National Science Foundation (Grants NSF OISE-1358175; PHY-1039130, PHY-1714833, No. IIA-1358175, PHY-2012940), INFN (Italy), and NSERC of Canada (Grant No. FRN-SAPPJ2015-00023). This infrastructure is part of a project that has received funding from the European Union's Horizon 2020 research and innovation programme under grant agreement No 824093.

References

[1] R.L. Workman, et al., Particle Data Group, Prog. Theor. Exp. Phys. 2022 (2022) 083C01.
[2] A. Thiel, F. Afzal, Y. Wunderlich, Prog. Part. Nucl. Phys. 125 (2022) 103949.
[3] D.G. Ireland, E. Pasyuk, I. Strakovsky, Prog. Part. Nucl. Phys. 111 (2020) 103752.
[4] Y. Wunderlich, F. Afzal, A. Thiel, R. Beck, Eur. Phys. J. A 53 (5) (2017) 86.
[5] N. Zachariou, et al., Phys. Lett. B 817 (2021) 136304.
[6] S. Strauch, et al., Phys. Lett. B 750 (2015) 53.
[7] https://pwa.hiskp.uni-bonn.de/Reaction_list.php.
[8] SAID database, http://gwdac.phys.gwu.edu/;
R.A. Arndt, et al., Phys. Rev. C 76 (2007) 025209.
[9] W.J. Briscoe, et al., Phys. Rev. C 100 (2019) 065205.
[10] A.V. Anisovich, et al., Eur. Phys. J. A 52 (2016) 284.
[11] D.P. Watts, J.R.M. Annand, M. Bashkanov, D.I. Glazier, MAMI Proposal Nr. A2/03-09, http://bamboo.pv.infn.it/Mambo/MAMI/prop_2009/MAMI-A2-03-09.pdf.
[12] K.-H. Kaiser, et al., Nucl. Instrum. Methods A 593 (2008) 159.
[13] J.C. McGeorge, et al., Eur. Phys. J. A 37 (2008) 129.
[14] A. Starostin, et al., Phys. Rev. C 64 (2001) 055205.
[15] S.J.D. Kay, Ph.D. thesis, University of Edinburgh, 2018.
[16] M. Bashkanov, et al., Phys. Rev. Lett. 124 (2020) 132001.
[17] M. Bashkanov, et al., arXiv:2206.12299.
[18] G. Audit, et al., Nucl. Instrum. Methods A 301 (1991) 473.
[19] M. Bashkanov, et al., Phys. Lett. B 789 (2019) 7.
[20] A.M. Sandorfi, et al., J. Phys. G, Nucl. Part. Phys. 38 (2011) 053001.
[21] A. Pastore, J. Phys. G 46 (2019) 052001.
[22] H. Olsen, L. Maximon, Phys. Rev. 114 (1959) 887.
[23] F. Cividini, et al., Eur. Phys. J. A 58 (6) (2022) 113.
[24] http://collaborations.fz-juelich.de/ikp/jedi/.
[25] F. Mueller, et al., Eur. Phys. J. A 56 (2020) 211.
[26] L. Hulthhn, M. Sugawara, in: S. Flugge (Ed.), Handbuch der Physik, vol. 39, Springer-Verlag, Berlin, 1957, p. 14.
[27] V.E. Tarasov, et al., Phys. Rev. C 84 (2011) 035203.
[28] W.J. Briscoe, A.E. Kudryavtsev, I.I. Strakovsky, V.E. Tarasov, R.L. Workman, Eur. Phys. J. A 58 (2) (2022) 23.
[29] M. Sikora, et al., Phys. Rev. Lett. 112 (2014) 022501.

[30] K. Wijesooriya, Phys. Rev. C 66 (2002) 034614.
[31] A.M. Sandorfi, et al., AIP Conf. Proc. 1432 (1) (2012) 219, arXiv:1108.5411, 2011.
[32] K.H. Althoff, et al., Nucl. Phys. B 131 (1977) 1.
[33] R.G. Edwards, et al., Phys. Rev. D 84 (2011) 074508.
[34] https://doi.org/10.15124/53c8fd02-4b3f-4fb9-908e-60c487d5615b.